20

Algorithm for identifying different forms of allogeneic collagen-containing material as a basis for bioink using optical analysis methods

© P.E. Timchenko[1,2], O.O. Frolov[1,2], N.A. Rjabov[2], E.V. Timchenko[1,2], L.T. Volova[2], S.S. Ivanov[1]

[1] Samara National Research University,
443086 Samara, Russia
[2] Samara State Medical University,
443099 Samara, Russia

e-mail: laser-optics.timchenko@mail.ru

Received November 30, 2023
Revised February 10, 2024
Accepted March 05, 2024

The results of a study assessing the composition of different forms of allogeneic collagen-containing material (hydrogel) as a potential component of bioink in a promising direction tissue engineering using optical methods (Raman and IR spectroscopy). As a result carried out studies using the Raman spectroscopy method, it was established that in non-hydrolyzed form of collagen, the relative content of proline and hydroxyproline is less than in the hydrolyzed form, which may indicate disturbances in the structural organization of collagen-containing material (according to the spectral features of proline and hydroxyproline). Based on analysis of variance there was an algorithm has been developed for identifying different forms of allogeneic collagen-containing material using decision tree. It has been established that using Raman and IR spectroscopy methods it is possible to carry out express analysis of the composition and types of collagen materials, as well as control the degree of denaturation collagen in the development of bioinks.

Keywords: Raman spectroscopy, IR spectroscopy, collagen identification algorithm, hydrogel, bioink, collagen-containing material, analysis of variance.

DOI: 10.61011/EOS.2024.04.58873.21-24

Introduction

The use of optical analysis techniques for qualitative and quantitative assessment of the composition of hydrogels [1] is a currently relevant aspect of tissue engineering (specifically, 3D bioprinting with regard to the development and analysis of bioinks). Bioinks may be based on materials of various origin. Allogeneic biomaterials, which are known to have a number of advantages (such as a low immune response, biomimeticity, and biodegradability [2,3]), are currently regarded as promising candidates for these applications. For example, scaffolds used in bone and cartilage tissue engineering should have an interconnected porous structure, fine biocompatibility, and mechanical properties matching the ones of their natural counterparts. Collagen-containing materials (collagen is the key component of the extracellular matrix [4,5]) are considered promising in this context.

An unbiased assessment of the quality of hydrogels and bioinks requires data on the structure of their components. Therefore, the evaluation of structural and qualitative characteristics and the state (hydrolyzed or non-hydrolyzed) of a collagen-containing material appears to be important.

Optical methods have been used in a number of studies [6,7].

Raman spectroscopy has several advantages over other optical methods, since it allows for prompt control and has a wide variety of uses in biomedical applications. Specifically, Raman spectroscopy has been used to examine the characteristics of the extracellular matrix in tissue samples. Raman spectroscopy has also been applied in bone marrow studies [8], and it has been found that the primary contributions to Raman spectra of bone marrow from BM-MSCs were produced by nucleic acids (isolated purine and/or pyrimidine bases and DNA/RNA structure), proteins (individual amino acids, amide groups of the secondary structure of proteins, and various vibrations within the C−C or C−N bonds), and lipids (vibrations within the hydrocarbon chain).

Thus, Raman spectroscopy is an efficient method for assessing cell populations and compositions of biomaterials.

Fourier-transform infrared spectroscopy, which is suited for rapid and high-quality chemical structural characterization of collagen properties [9], is no less promising than Raman spectroscopy. This method is also used widely, since it allows for precise determination of the chemical structural properties of collagen from various sources. Using a non-destructive technique such as FTIR, one may obtain valuable molecular-level data on the types of functional groups, types of bonds and molecular conformations, and characterize easily and distinguish the quality of collagen-based biomaterials in human biological tissues [10]. This was confirmed by the authors of literature review [11], where the application of FTIR for the examination of collagen-based biomaterials extracted from various sources and for the characterization of collagen-based materials used in wound

healing, as skin substitutes and collagen-containing drug delivery agents, in tissue engineering, bone regeneration, osteogenic differentiation, etc., was highlighted.

The aim of the present study was to perform Raman and FTIR analysis for evaluating the composition of different forms of a collagen-containing material intended to be used as a basis for bioinks.

Materials and research techniques

The following two groups of samples were examined:

group 1 — collagen-containing material, non-hydrolyzed form;

group 2 — collagen-containing material, hydrolyzed form.

The starting material for production of the collagen-containing material was mineralized allogeneic spongy bone tissue, which was cleaned of blood, lipids, bone marrow stroma, and other components using the patented original „Lioplast“ technology ® (TU-9398-001-01963143-2004) with subsequent lyophilization. Demineralized tissue was then obtained from mineralized bone tissue by removing the bone mineral component (BMC) (hydroxyapatite) chemically. The next step was to prepare a gel form or hydrogel of the collagen-containing material from demineralized bone tissue by extracting the protein complex with acid and neutralizing the resulting gel with alkali. A buffer solution was added to maintain a stable hydrogel pH value. The obtained hydrogel was of medium viscosity, slow-flowing, and transparent; its pH value was 7.2–7.4. The next step was lyophilization of this hydrogel (preparation of a lyophilisate). Collagen hydrolysate was obtained enzymatically using the trypsin enzyme (OOONPP „PanEco,“ trypsin 1:250, activity: 349 U/mg, Cat. No. P032, WA200226).

Raman spectroscopy was performed on a test stand [12] fitted with a semiconductor laser (LML-785.0RB-04,450 MW), a spectrograph (SharmrockSR-303i) with an integrated digital camera cooled to −60°C, an optical Raman module (PBL785), and a computer.

The SharmrockSR-303i spectrograph provides a wavelength resolution of 0.15 nm at a low level of intrinsic noise. Raman spectra were recorded with an optical probe [13].

The obtained spectra were processed [14]. The spectral analysis was confined to the $450-1800\,cm^{-1}$ range. Normalization and smoothing of the Raman spectra were performed using the SNV and Maximum Likelihood Estimation Savitzky–Golay filtering (MLE-SG) (= 4) methods.

The method of subtracting the fluorescence component by the I-ModPoly polynomial approximation with a polynomial degree of 11 was used to filter out autofluorescence from the Raman spectra.

Fourier IR spectroscopy of samples was utilized as an additional biomaterial analysis technique. An FT-801 instrument („SIMEX,“ Russia) was used in these experiments. IR spectra of samples were recorded using a multiple-reflection ATR (attenuated total reflection) accessory with a zinc selenide element. The reflection method (with three reflections) and the ZaIR3.5 software were used. The measurement resolution was $4\,cm^{-1}$, and the range was $500-4000\,cm^{-1}$.

IR spectra are used to identify compounds and determine the degree of their purity (qualitatively); they are also suitable for qualitative analysis of mixtures in monitoring the progress of a reaction. However, the prevalent and most important mode of application of IR spectra is the clarification and verification of the tentative structure of compounds. The mentioned instrument allows one to determine the presence of almost any functional group in a molecule.

Results

Figure 1 shows the averaged normalized Raman spectra of the samples under study.

It can be seen that the hydrolyzed form of collagen is characterized by high intensities of Raman lines in the $800-1464\,cm^{-1}$ spectral range; the most notable Raman lines in the spectra of this sample are those at 854 and $876\,cm^{-1}$ (C–C stretching, proline and hydroxyproline (collagen assignment)), $1003/1036\,cm^{-1}$ (Phenylalanine (Breathing mode) (collagen assignment)), $1094\,cm^{-1}$ (Phospholipids), $1270\,cm^{-1}$ (Amide III/α-helix), $1449\,cm^{-1}$ (CH_2 bending and scissoring modes of collagen and phospholipids).

The authors of [15] have noted that the relative amount of proline ($854\,cm^{-1}$ in the Raman spectra) affects collagen synthesis directly, since the most important stage in protein synthesis (post-translational modification) follows on the chemical reaction of proline hydroxylation. In its hydrolyzed form, the collagen-containing allogeneic material preserves a complex of amino acids (the key protein components of bone tissue: proline, phenylalanine, hydroxyproline) that are used by the body as building blocks in the process of collagen synthesis when the implanted structure is substituted by the body's own tissues.

Optical methods allow one to evaluate the quality of the hydrolyzed collagen-containing material by verifying the preservation of the complex of essential amino acids.

Thus, changes in the percentage of proline and hydroxyproline may serve as indicators of the biomaterial quality.

An increase in the concentration of hydroxyproline (the $854\,cm^{-1}$ line), which is a part of the collagen protein and is associated with bone matrix peptides, in the hydrolyzed form of collagen may be indicative of suppression of resorptive processes [16].

The wave number of $1036\,cm^{-1}$ corresponds to vibrations in the phenylalanine molecule [17]. This amino acid is relevant to the study of osteoresorption, since it is also involved in the process of collagen synthesis and governs such properties of collagen fibrils as elasticity and resilience. The intensity of the line at this wave number decreases in the spectra of non-hydrolyzed collagen.

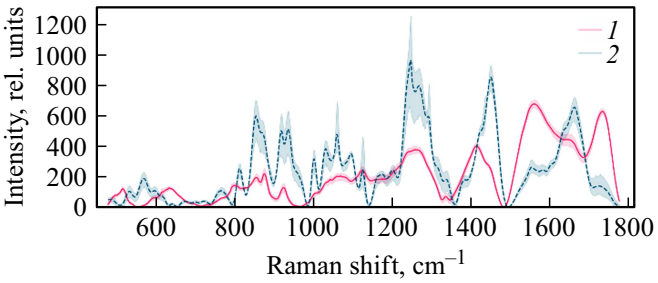

Figure 1. Averaged normalized Raman spectra of the samples under study: group 1 (red curve); group 2 (blue curve).

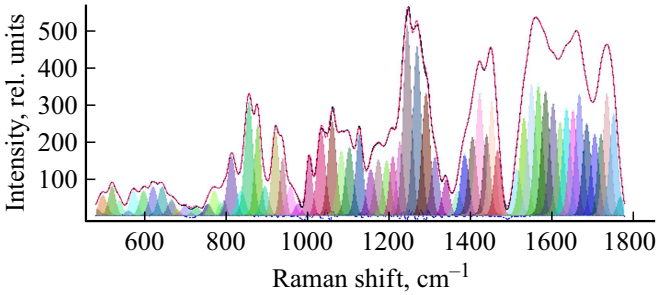

Figure 2. Resulting model of decomposition of the Raman spectrum by Voigt lines (black solid curve — original spectrum; red dotted curve — simulated spectrum; blue dotted curve — difference between the original and simulated spectra).

The most significant differences between the two examined groups are found in the 1559–1736 cm^{-1} spectral region. Specifically, the hydrolyzed form of collagen features a peak at 1663 cm^{-1} (Amide I/α-helix), which is fairly faint in the spectrum of non-hydrolyzed collagen. At the same time, the lines at 1559 cm^{-1} (amid II Parallel/Antiparallel β-sheet structure) and 1736 cm^{-1} (phospholipids) are the most pronounced in the non-hydrolyzed form of collagen.

In order to extract more information from the obtained Raman spectra, they were decomposed (Fig. 2) into a sum of 66 spectral Voigt profile lines characterized by formula (1). The composition of spectral lines was determined by automatic multi-iteration modeling of 21 Raman spectra.

$$f(x;A,x_0,\sigma,a) = \frac{(1-\alpha)A}{\sigma_g\sqrt{2\pi}}e^{\left[-(x-x_0)^2/2\sigma_g^2\right]} + \frac{\alpha A}{\pi}\left[\frac{\sigma}{(x-x_0)^2+\sigma^2}\right], \qquad (1)$$

where $\sigma_g = \sigma/\sqrt{2\ln 2}$ is the FWHM value, A is the amplitude, α is the coefficient setting the relative weight of Gaussian and Lorentzian components ($\sigma = 0$ and $\alpha = 1$ correspond to Gaussian and Lorentzian profiles, respectively), and x_0 is the position of the line maximum.

The limited-memory BFGS (L-BFGS-B) method was used to optimize the model. The average values of parameters of the Raman spectra obtained as a result of decomposition were as follows: $R^2 = 99.68\%$, $\chi^2 = 11640$, $aic = 633$, $bic = 849$.

The line amplitudes obtained after decomposition were analyzed using ANOVA (analysis of variance). The amplitudes of seven most informative lines are shown in Fig. 3.

The distribution of amplitude of any of these seven lines allows one to distinguish clearly between the spectra of the 1st and 2nd groups; therefore, all these lines may be used to construct a decision tree. The most significant differences are observed in the amplitude distribution for the ~ 1736 cm^{-1} Raman line (phospholipids).

With the analysis of variance factored in, one may establish the criterion for differentiation between the spectra of groups 1 and 2 based on a single line with the use of a decision tree (Fig. 4). If the line amplitude is below 284.265 rel. units, the examined Raman spectrum corresponds to the hydrolyzed form of collagen.

The primary functional groups characteristic of the collagen structure are found in the FTIR spectra of the non-hydrolyzed collagen-containing material (Fig. 5) (Group 2). The FTIR spectrum features peaks corresponding to amide I (1631 cm^{-1}), amide II (N–H group bending at 1534 cm^{-1}), and amide III stretching vibrations at 1231 cm^{-1}. A pronounced hydroxyl band in the region of 3300 cm^{-1}, which corresponds to the stretching vibrations of N–H, is also seen. One may also note the presence of -COOH and -OH groups that are characterized by the peaks at 1739, 1645, and 1073 cm^{-1} [18]. In light of literature data [19], this verifies the presence of a collagen structure in the sample under study.

In the hydrolyzed form of the collagen-containing material (Group 2), the intensity of the amide I and amide III peaks and the vibration of proline side chains present in the collagen-containing material (1325–1340 cm^{-1}) decreases after enzymatic treatment. This is indicative of unfolding of triple helices due to collagen denaturation. The triple helical structure of collagen is verified by the intensity of the peak characteristic of amide III at 1447 cm^{-1}.

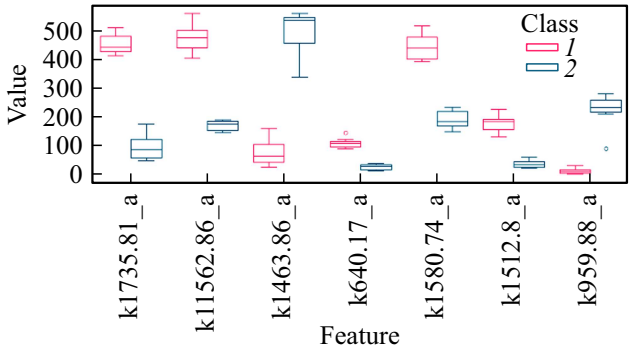

Figure 3. Amplitudes of the most informative lines: *1* — first group; *2* — second group.

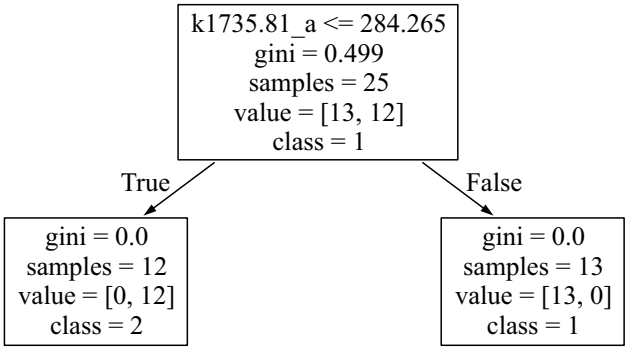

Figure 4. Decision tree.

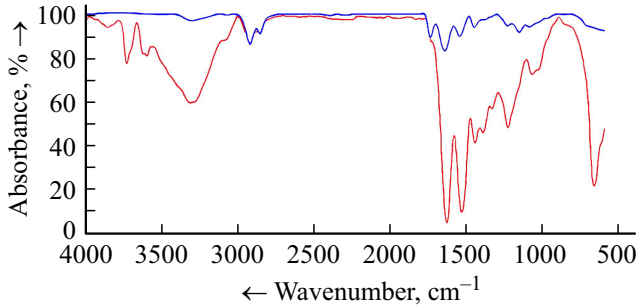

Figure 5. Averaged FTIR spectra of the studied samples: group *1* — non-hydrolyzed form of the collagen-containing material (red curve); group *2* — hydrolyzed form of the collagen-containing material (blue curve).

Conclusion

Raman spectroscopy data revealed that the percentage of proline and hydroxyproline in the non-hydrolyzed form of collagen is lower than in the hydrolyzed form. This may be indicative of abnormalities in the processes of collagen synthesis. At the same time, an increase in the concentration of hydroxyproline (the 854 cm^{-1} line), which is a part of the collagen protein and is associated with bone matrix peptides, in the hydrolyzed form of collagen suggests a possible suppression of resorptive processes.

The results of mathematical processing of Raman spectra demonstrated that the greatest difference in the distribution of line amplitudes is observed for the $\sim$ 1736 cm^{-1} (phospholipids) line.

An algorithm for identifying different forms of collagen for bioinks with the use of a decision tree was developed based on the analysis of variance. It was demonstrated that if the amplitude of the 1736 cm^{-1} Raman line is below 284.265 rel. units, the examined spectrum is the one of a lyophilized gel of hydrolyzed collagen.

The FTIR method was used successfully to characterize the peaks of the non-hydrolyzed collagen-containing material sample corresponding to amide I (1631 cm^{-1}), amide II (1534 cm^{-1}), and amide III (1447 cm^{-1}). It was found that the intensity of these peaks increases significantly (due presumably to the denaturation of collagen) when the sample becomes hydrolyzed.

Thus, a combination of two optical non-destructive screening methods — IR and Raman spectroscopy — provides an opportunity to perform qualitative express analysis of the composition and types of collagen in the course of development of bioinks for 3D bioprinting with the use of biological materials.

Conflict of interest

The authors declare that they have no conflict of interest.

References

[1] R. Tehseen, Z. Rabia, Z. Faiza, I. Kanwal, M. Nawshad, S.S. Zaman, A. Rahim, S.A.A. Rizvi, I.U. Rehman. Appl. Spectrosc. Rev., **53** (9), 703 (2018). DOI: 10.1080/05704928.2018.1426595
[2] D.F. Williams. Biomater., **29** (20), 2941 (2008). DOI: 10.1016/j.biomaterials.2008.04.023
[3] S. Prokoshkin, Y. Pustov, Y. Zhukova, P. Kadirov, S. Dubinskiy, V. Sheremetyev, M. Karavaeva. Materials, **52**, 2024 (2021). DOI: 10.3390/ma14123327
[4] T. Long, J. Yang, S.S. Shi, Y.P. Guo, Q.F. Ke, Z.A. Zhu. J. Biomed. Mater. Res. B. Appl. Biomater., (7), 1455 (2015). DOI: 10.1002/jbm.b.33328
[5] M.B. Fauzi, Y. Lokanathan, B.S. Aminuddin, B.H.I. Ruszymah, S.R. Chowdhury. Mater. Sci. Eng. C. Mater. Biol. Appl., **68**, 163 (2016). DOI: 10.1016/j.msec.2016.05.109
[6] G.I. Dolgikh, V.E. Privalov. *Lazernaya fizika. Fundamental'nye i prikladnye issledovaniya* (OOO „Reya,"Vladivostok, 2016) (in Russian).
[7] G.V. Laktyushkin, V.E. Privalov., V.G. Shemanin. Tech. Phys., **43** (1), 16 (1998).
[8] M. Jackson, L.P. Choo, P.H. Watson, W.C. Halliday., H.H. Mantsch. Biochimica et Biophysics Acta, **1270** (1), 1 (1995) DOI: 10.1016/0925-4439(94)00056-v
[9] H.L. Casal, H.H. Mantsch. Biochim. Biophys. Acta, **779** (4), 381 (1984). DOI: 10.1016/0304-4157(84) DOI: 10.1016/0304-4157(84)90017-0
[10] M. Jackson, H.H. Mantsch. Spectrochim. Acta Rev., **15**, 53 (1993).
[11] E.V. Timchenko, P.E. Timchenko, E.V. Pisareva, M.A. Daniel, L.T. Volova, A.A. Fedotov, O.O. Frolov, A.N. Subatovich. J. Opt. Technology, **87** (3), 161 (2020). DOI: 10.1364/JOT.87.000161
[12] P.E. Timchenko, E.V. Timchenko, L.T. Volova, M.A. Zybin, O.O. Frolov, G.G. Dolgushov. Optical Memory and Neural Networks, **29** (4), 354 (2020).
[13] P.E. Timchenko, E.V. Timchenko, L.T. Volova, O.O. Frolov. J. Opt. Technology, **88** (9), 485 (2021). DOI: 10.1364/JOT.88.000485
[14] R.H. Christenson. Clinical biochemistry, **30** (8), 573 (1997). DOI: 10.1016/S0009-9120(97)00113-6
[15] W.J. Marshall, M. Lapsley, A.P. Day, R.M. Ayling. *Clinical Biochemistry: Metabolic and Clinical Aspects: Third Edition* (2014).
[16] R. Polak, R.N. Pitombo. Cryobiology, **63** (2), 61 (2011).

[17] T. Mitra, G. Sailakshmi, A. Gnanamani. Proceedings of the Indian Academy of sciences. Chemical sciences, **126** (1), 127 (2014). DOI: 10.1007/s12039-013-0543-2.
[18] B. Dong, O. Arnoult, M.E. Smith, G. Wnek. Macromol Rapid Commun., **30** (7), 539 (2009). DOI: 10.1002/marc.200800634.
[19] S.J. Kew, J.H. Gwynne, D. Enea, R. Brookes, N. Rushton. Acta Biomater., **8** (10), 3723 (2021). DOI: 10.1016/j.actbio.2012.06.018

Translated by D.Safin